

Minimal Higgs inflation

Yuta Hamada,^{*} Hikaru Kawai,[†] and Kin-ya Oda[‡]

^{*†}*Department of Physics, Kyoto University, Kyoto 606-8502, Japan*

[‡]*Department of Physics, Osaka University, Osaka 560-0043, Japan*

December 17, 2013

Abstract

We consider a possibility that the Higgs field in the Standard Model (SM) serves as an inflaton when its value is around the Planck scale. We assume that the SM is valid up to an ultraviolet cutoff scale Λ , which is slightly below the Planck scale, and that the Higgs potential becomes almost flat above Λ . Contrary to the ordinary Higgs inflation scenario, we do not assume the huge non-minimal coupling, of $O(10^4)$, of the Higgs field to the Ricci scalar. We find that Λ must be less than 5×10^{17} GeV in order to explain the observed fluctuation of the cosmic microwave background, no matter how we extrapolate the Higgs potential above Λ . The scale 10^{17} GeV coincides with the perturbative string scale, which suggests that the SM is directly connected with the string theory. For this to be true, the top quark mass is restricted to around 171 GeV, with which Λ can exceed 10^{17} GeV. As a concrete example of the potential above Λ , we propose a simple log type potential. The predictions of this specific model for the e -foldings $N_* = 50$ – 60 are consistent with the current observation, namely, the scalar spectral index is $n_s = 0.977$ – 0.983 and the tensor to scalar ratio $0 < r < 0.012$ – 0.010 . Other parameters, $dn_s/d \ln k$, n_t , and their derivatives, are also consistent.

^{*}E-mail: hamada@gauge.scphys.kyoto-u.ac.jp

[†]E-mail: hkawai@gauge.scphys.kyoto-u.ac.jp

[‡]E-mail: odakin@phys.sci.osaka-u.ac.jp

1 Introduction

It is more and more plausible that the particle discovered at the CERN Large Hadron Collider (LHC) [1, 2] around 126 GeV is the Standard Model (SM) Higgs boson. Its couplings to the W and Z gauge bosons, to the top and bottom quarks, and to the tau lepton are all consistent to those in the SM within one standard deviation even though their values vary two orders of magnitude, see e.g. Ref. [3]. No hint of new physics beyond the SM has been found so far at the LHC up to 1 TeV. It is important to examine up to what scale the SM can be a valid effective description of nature.

The determination of the Higgs mass finally fixes all the parameters in the SM. We can now obtain the *bare* parameters at Λ . These parameters are important. If a ultraviolet (UV) theory such as string theory fails to fit them, it is killed.

The parameters in the SM are dimensionless except for the Higgs mass (or equivalently its vacuum expectation value (VEV)). The dimensionless bare coupling constants can be approximated by the running ones at Λ , see e.g. Appendix of Ref. [4]. Once the low energy inputs are given, we can evaluate the running couplings through the renormalization group equations (RGEs) of the SM. The detailed RGE study of the SM tells us that both the Higgs quartic coupling and its beta function become tiny at the same scale $\sim 10^{17}$ GeV for the input value of the Higgs mass around 126 GeV; see e.g. Refs. [5, 6, 7, 8, 9, 4, 10, 11] for latest analyses.

After fixing all the dimensionless bare couplings, the last remaining parameter in the SM is the bare Higgs mass. The quadratically divergent bare Higgs mass is found to be suppressed too when the UV cutoff is $\Lambda \gtrsim 10^{17}$ GeV [4]; see also Refs. [10, 12, 13, 14], and also Refs. [15, 16, 17, 18, 19]. The absence of the bare mass at Λ , along with the vanishing quartic coupling and its beta function, implies that the Higgs potential is approximately flat there and that its height is suppressed compared to (the fourth power of) the cutoff scale.

Following the evidence of the top quark with mass $174 \pm 10_{-12}^{+13}$ GeV [20] in 1994, Froggatt and Nielsen have predicted [21] that the top and Higgs masses are 173 ± 5 GeV and 135 ± 9 GeV, respectively. This prediction is based on the multiple point principle (MPP) that the SM Higgs potential must have another minimum at the Planck scale and that its height is (order-of-magnitude-wise [22, 23]) degenerate to the SM one. This assumption is equivalent to the vanishing Higgs quartic coupling and its beta function at the Planck scale. The success of this prediction indicates that at least the top-Higgs sector of the SM remains unaltered up to a very high UV cutoff scale Λ .¹

In the MPP, it is assumed that there are two vacua that are separated by a potential barrier, as illustrated in the lowermost (green) solid and dashed lines in Fig. 2. In this paper, we consider the case where there is no potential barrier, as illustrated in the middle (blue) and uppermost (red) lines in Fig. 2 so that the Higgs potential can be used for an inflation. In order to have an inflation consistent with the current observational data, we assume that the low energy SM

¹ As a possible modification, the classically conformal $B-L$ model is considered in [24, 25, 26]. This model can realize the flat potential at the Planck scale and solve the hierarchy problem [27].

Higgs potential, depicted by the solid lines, is smoothly connected to an almost flat potential, depicted by the dot-dashed lines, around the UV cutoff scale Λ .²

Some of the concrete examples of the flat potential above the cutoff are the following: In the gauge-Higgs unification scenario, the potential for $\langle A_5 \rangle$ is almost flat for large field values $\langle A_5 \rangle \gg R^{-1}$ because of the gauge invariance and is bounded from above by $O(R^{-4})$ [28]; similar mechanism can be expected in string compactification [29, 30]; see also Refs. [31, 32, 33, 34, 35]. Another example is the Coleman-Weinberg potential [36] with an explicit momentum cutoff Λ . For a field value beyond Λ , we get a log potential, as we explain in Appendix B. (This possibility is pursued in Section 4.2.)

The latest cosmological data [37] constrains the scalar fluctuation amplitude A_s , the spectral index n_s , the tensor-to-scalar ratio r ; see also Ref. [38] for a recent review. By assuming the slow-roll inflation, these values are completely fixed by the potential height \mathcal{V}_* and its derivatives \mathcal{V}'_* and \mathcal{V}''_* at a field value φ_* corresponding to a given e -folding $N_* \simeq 60$. If we allow arbitrary shape of the Higgs potential in all the range beyond the electroweak scale, we can trivially satisfy these constraints. In our case, however, the SM potential in the range $\varphi < \Lambda$ is fixed by the known SM parameters. In order to avoid the graceful exit problem [39, 40, 41], the potential must be monotonically increasing in the entire region, both below and above Λ . In particular, the value of the SM potential at the cutoff must satisfy $\mathcal{V}_{\text{SM}}(\varphi = \Lambda) < \mathcal{V}_*$. As a result, we get an upper bound: $\Lambda \lesssim 10^{17}$ GeV, when the top quark mass is $M_t \lesssim 171$ GeV, irrespectively of the extrapolation of the potential above the cutoff $\varphi > \Lambda$.

As said above, we propose a possible extrapolation of the potential beyond Λ , log plus constant, motivated by the Coleman-Weinberg potential with the cutoff Λ . We show predictions of the spectral indices, their derivatives, etc. of the cosmic microwave background (CMB) in this model.

Our scenario differs from the conventional Higgs inflation scenario [42, 43, 44, 45, 46, 47], which achieves the flatness of the Higgs potential by the huge Higgs coupling to the Ricci scalar: $\xi |\phi|^2 \mathcal{R}$ with $\xi \sim 10^4$. The idea of the Higgs inflation is attractive, but it would be even better if we can realize it without such a coupling to gravity. See also Ref. [48, 49] for the unitarity issue of the conventional Higgs inflation, which necessitates new particles above M_P/ξ .³

This paper is organized as follows. In Section 2, we review the constraints from the cosmological observations including the latest results from the Planck experiment. In Section 3, we present the RGE running of the dimensionless couplings in the SM in the modified minimal subtraction ($\overline{\text{MS}}$) scheme; we also show the bare Higgs mass-squared parameter at Λ . Then we show that the SM Higgs potential can become flat around 10^{17} GeV. In Section 4, we examine a necessary condition that the Higgs field in the SM can serve as an inflaton assuming arbitrary shape

² In the original argument of the MPP [21], the partition function has been maximized as a function of the bare Higgs mass. In more recent Ref. [23], Nielsen has generalized their argument and considered several possibilities of the function to be maximized. In the context of Ref. [23], our approach could be regarded as the maximization of the entropy of the universe by requiring the occurrence of the inflation.

³ The authors of Refs. [50, 51] have proposed a Higgs inflation model in which the Higgs kinetic term is modified; the unitarity issue of this scenario, which involves higher derivatives of the Higgs field, would also be interesting to study.

of potential above Λ . In the last section, we summarize our results.

2 Constraints on inflation models

We briefly review and summarize our notation on the cosmological constraints from the CMB data observed at the Planck experiment, basically following Ref. [37]. The curvature and tensor power spectra are expanded around a pivot scale k_* as

$$\mathcal{P}_{\mathcal{R}} = A_s \left(\frac{k}{k_*} \right)^{n_s - 1 + \frac{1}{2} \frac{dn_s}{d \ln k} \ln \frac{k}{k_*} + \frac{1}{3!} \frac{d^2 n_s}{d \ln k^2} \left(\ln \frac{k}{k_*} \right)^2 + \dots}, \quad \mathcal{P}_t = A_t \left(\frac{k}{k_*} \right)^{n_t + \frac{1}{2} \frac{dn_t}{d \ln k} \ln \frac{k}{k_*} + \dots}. \quad (1)$$

We take the slow-roll approximation hereafter. The slow-roll parameters at a given position φ of the inflaton potential \mathcal{V} are defined as

$$\epsilon_V = \frac{M_P^2}{2} \frac{\mathcal{V}_\varphi^2}{\mathcal{V}^2}, \quad \eta_V = M_P^2 \frac{\mathcal{V}_{\varphi\varphi}}{\mathcal{V}}, \quad \xi_V^2 = M_P^4 \frac{\mathcal{V}_\varphi \mathcal{V}_{\varphi\varphi\varphi}}{\mathcal{V}^2}, \quad \varpi_V^3 = M_P^6 \frac{\mathcal{V}_\varphi^2 \mathcal{V}_{\varphi\varphi\varphi\varphi}}{\mathcal{V}^3}. \quad (2)$$

The number of e -folding before the end of inflation t_{end} from a time t_* becomes

$$N_* = \int_{t_*}^{t_{\text{end}}} dt H = \int_{\varphi_*}^{\varphi_{\text{end}}} \frac{d\varphi}{\dot{\varphi}} H = \frac{1}{M_P^2} \int_{\varphi_{\text{end}}}^{\varphi_*} \frac{\mathcal{V}}{\mathcal{V}_\varphi} d\varphi = \frac{1}{M_P} \int_{\varphi_{\text{end}}}^{\varphi_*} \frac{d\varphi}{\sqrt{2\epsilon_V}}, \quad (3)$$

where we have taken $\mathcal{V}_\varphi > 0$ in the last step. The end of inflation is defined by the field value φ_{end} below which the slow roll condition is violated:

$$\max \left\{ \epsilon_V(\varphi_{\text{end}}), |\eta_V(\varphi_{\text{end}})| \right\} = 1. \quad (4)$$

For most reasonable inflation models, the scale that we are observing from the CMB data corresponds to the e -folding in the range [37]

$$50 < N_* < 60. \quad (5)$$

In the following, we evaluate the slow-roll parameters at φ_* that satisfies Eq. (5). (We will also consider the range $40 < N_* < 50$ in Section 4.2 for comparison.)

The cosmological parameters are given by⁴

$$A_s = \frac{\mathcal{V}}{24\pi^2 M_P^4 \epsilon_V}, \quad A_t = \frac{2\mathcal{V}}{3\pi^2 M_P^4}, \quad r = \frac{A_t}{A_s} = 16\epsilon_V, \quad (6)$$

$$\begin{aligned} n_s &= 1 + 2\eta_V - 6\epsilon_V, & n_t &= -2\epsilon_V, \\ \frac{dn_s}{d \ln k} &= 16\epsilon_V \eta_V - 24\epsilon_V^2 - 2\xi_V^2, & \frac{dn_t}{d \ln k} &= -4\epsilon_V \eta_V + 8\epsilon_V^2, \\ \frac{d^2 n_s}{d \ln k^2} &= -192\epsilon_V^3 + 192\epsilon_V^2 \eta_V - 32\epsilon_V \eta_V^2 \\ &\quad - 24\epsilon_V \xi_V^2 + 2\eta_V \xi_V^2 + 2\varpi_V^3, \end{aligned} \quad (7)$$

⁴ Eq. (17) of Ref. [37] contains a typo (an overall wrong sign for $dn_s/d \ln k$). Also note that in the case of $\Lambda\text{CDM}+r+dn_s/d \ln k$ in Table 5 of Ref. [37], there is missing minus in front of the mean value of the $dn_s/d \ln k$ for Planck+WP and Planck+WP+lensing. We thank the referee for bringing this point to our attention and Finelli Fabio for his kind clarification.

where the quantities are evaluated at the field value φ_* .

At the pivot scale $k_* = 0.05 \text{ Mpc}^{-1}$, the scalar amplitude A_s and the spectral index n_s are constrained by the Planck+WMAP data as [37]

$$A_s = (2.196_{-0.060}^{+0.051}) \times 10^{-9}, \quad (8)$$

$$n_s = 0.9603 \pm 0.0073, \quad (9)$$

assuming $dn_s/d \ln k = d^2 n_s/d \ln k^2 = r = 0$.

If we include the tensor-to-scalar ratio r as an extra parameter, the Planck+WMAP+high- ℓ data [37] at the pivot scale $k_* = 0.002 \text{ Mpc}^{-1}$ give the 1σ range for n_s and the 95% CL limit on r as

$$n_s = 0.9600 \pm 0.0071, \quad r < 0.11. \quad (10)$$

On the other hand, if we include $dn_s/d \ln k$ as an extra parameter, we obtain the constraint at the pivot scale $k_* = 0.05 \text{ Mpc}^{-1}$ [37]

$$n_s = 0.9561 \pm 0.0080, \quad \frac{dn_s}{d \ln k} = -0.0134 \pm 0.0090. \quad (11)$$

One may vary both r and $dn_s/d \ln k$ to fit the Planck+WMAP data at the pivot scale $k_* = 0.05 \text{ Mpc}^{-1}$, and obtains [37]

$$n_s = 0.9583 \pm 0.0081, \quad r < 0.25, \quad \frac{dn_s}{d \ln k} = -0.021 \pm 0.012, \quad (12)$$

where the constraint on r is given at 95% CL.⁵

We note that the upper bound on r gives that of the inflaton energy scale [37]

$$\mathcal{V}_{\max} = \frac{3\pi^2 A_s}{2} r_{\max} M_P^4 = 1.3 \times 10^{65} \text{ GeV}^4 \times \left(\frac{r_{\max}}{0.11} \right). \quad (13)$$

3 SM Higgs potential

The SM Higgs potential much above the electroweak scale but below the cutoff scale Λ is governed by the RGE running of the Higgs quartic coupling λ , which highly depends on the top Yukawa coupling y_t . Therefore we first review how y_t is determined; then we show the numerical results of the RGEs; finally we present the resultant Higgs potential around Λ .

⁵ In terms of the slow-roll parameters, these conditions become

$$\epsilon_V < 0.015, \quad \eta_V = -0.014_{-0.011}^{+0.015}, \quad |\xi_V^2| = 0.009 \pm 0.006.$$

where the constraint on ϵ_V is given at 95% CL.

3.1 Coupling constants at the electroweak scale

The most precise determination of the top quark mass is given by a combination of the Tevatron data for the invariant mass of the top quark decay products [52]:

$$M_t^{\text{inv}} = 173.20 \pm 0.87 \text{ GeV}. \quad (14)$$

The problem of the Tevatron determination (14) is that the invariant mass, which is reconstructed from the color singlet final states, cannot be the pole mass of the colored top quark [8]. Instead, the authors of Ref. [8] proposed to get the top mass by fitting the $t\bar{t} + X$ inclusive cross section, and obtained the pole mass:⁶

$$M_t = 173.3 \pm 2.8 \text{ GeV}. \quad (15)$$

The numerical value of the $\overline{\text{MS}}$ Yukawa coupling at the top mass scale can be read off from Ref. [7] as

$$y_t(M_t) = 0.93669 + 0.01560 \left(\frac{M_t - 173.3 \text{ GeV}}{2.8 \text{ GeV}} \right) - 0.00041 \left(\frac{\alpha_s(M_Z) - 0.1184}{0.0007} \right) - 0.00001 \left(\frac{M_H - 125.6 \text{ GeV}}{0.4 \text{ GeV}} \right) \pm 0.00200_{\text{th}}, \quad (16)$$

where we have employed a combined Higgs mass $M_H = 125.6 \pm 0.4 \text{ GeV}$. The electroweak gauge couplings at the Z mass scale are [59]

$$g_Y(M_Z) = 0.357418(35), \quad g_2(M_Z) = 0.65184(18). \quad (17)$$

The $\overline{\text{MS}}$ strong and quartic couplings at the top mass scale are [7]

$$g_s(M_t) = 1.1644 + 0.0031 \left(\frac{\alpha_s(M_Z) - 0.1184}{0.0007} \right) - 0.0013 \left(\frac{M_t - 173.3 \text{ GeV}}{2.8 \text{ GeV}} \right), \quad (18)$$

$$\lambda(M_t) = 0.12699 + 0.00082 \left(\frac{M_H - 125.6 \text{ GeV}}{0.4 \text{ GeV}} \right) - 0.00012 \left(\frac{M_t - 173.3 \text{ GeV}}{2.8 \text{ GeV}} \right) \pm 0.00140_{\text{th}}. \quad (19)$$

3.2 Numerical Results of SM RGEs

We use the two-loop RGEs in the SM which are summarized in Ref. [4]. We show our result of running $\overline{\text{MS}}$ couplings in Fig. 1. The gauge couplings g_Y , g_2 , g_3 are drawn by thick lines. The thickness of the curves for y_t , λ and β_λ comes from the

⁶ As clarified in Refs. [53, 54], currently there are two ways to define the $\overline{\text{MS}}$ running top mass for a given $\overline{\text{MS}}$ running Yukawa $y_t(\mu)$. The $\overline{\text{MS}}$ mass used in QCD [55, 56, 8], which we call $m_t^{\text{QCD}}(\mu)$, can be approximately written as $m_t^{\text{QCD}}(\mu) \simeq y_t(\mu)V/\sqrt{2}$ with $V = 246.22 \text{ GeV}$, up to electroweak corrections less than 1%. In Refs. [57, 58], $\overline{\text{MS}}$ mass is defined as $m_t(\mu) := y_t(\mu)v(\mu)/\sqrt{2}$, where $v(\mu)$ is given by the relation $-m^2(\mu) = \lambda(\mu)v^2(\mu)$, with $m^2(\mu)$ being the running mass parameter in the tree potential in the $\overline{\text{MS}}$ scheme: $\mathcal{V} = m^2(\mu)\phi^\dagger\phi + \lambda(\mu)(\phi^\dagger\phi)^2$. There are $\sim 7\%$ difference between $m_t^{\text{QCD}}(M_t)$ and $m_t(M_t)$ [58], which is mainly due to the tadpole contribution from the top quark. Though the bound on the pole mass (15) has been derived from that on $m_t^{\text{QCD}}(M_t) = 163.3 \pm 2.7 \text{ GeV}$ [8], it is consistent to use Eq. (15) in obtaining the Yukawa coupling (16) since the pole mass M_t should be the same in both schemes.

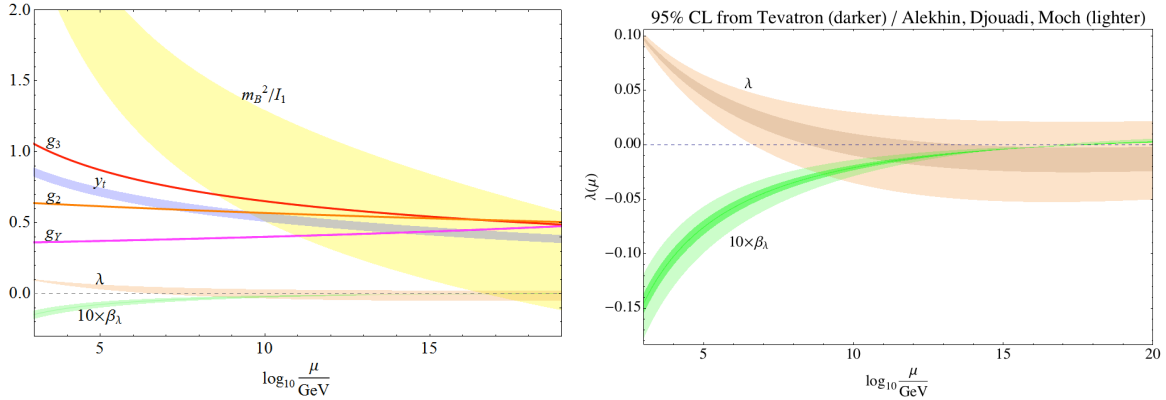


Figure 1: Left: $\overline{\text{MS}}$ running couplings. The 95% confidence intervals are given for m_B^2/I_1 , $y_t(\mu)$, $\lambda(\mu)$, and $10\beta_\lambda(\mu)$; see text for more details. The intervals for the gauge couplings g_Y , g_2 , and g_3 are too small to be seen. Right: Enlarged view around the horizontal axis of Left. Darker bands are the 95% confidence intervals under the (theoretically unjustified) assumption that the Tevatron mass (14) can be identified with the top pole mass M_t .

1.96 σ variation of M_t (15), where $\alpha_s(M_Z)$ and M_H are fixed to their central values. Similarly, we plot the bare Higgs mass-squared m_B^2 , divided by the quadratically divergent integral $I_1 = \Lambda^2/16\pi^2$, as a function of Λ [4, 53]. Note that the bare mass m_B^2 is *not* the running mass.

We see that the Higgs quartic coupling λ has a minimum around 10^{17} GeV. This is due to the fact that the beta function of λ receives less negative contribution from the top loop since y_t becomes smaller at high scales.

We can fit the parameters at the reduced Planck scale⁷ $M_P := 1/\sqrt{8\pi G} = 2.4 \times 10^{18}$ GeV as

$$\lambda(M_P) = -0.015 - 0.019 \left(\frac{M_t - 173.3 \text{ GeV}}{2.8 \text{ GeV}} \right) + 0.002 \left(\frac{\alpha_s(M_Z) - 0.1184}{0.0007} \right) + 0.001 \left(\frac{M_H - 125.6 \text{ GeV}}{0.4 \text{ GeV}} \right), \quad (20)$$

$$\frac{m_B^2}{M_P^2/16\pi^2} = 0.26 + 0.18 \left(\frac{M_t - 173.3 \text{ GeV}}{2.8 \text{ GeV}} \right) - 0.02 \left(\frac{\alpha_s(M_Z) - 0.1184}{0.0007} \right) - 0.01 \left(\frac{M_H - 125.6 \text{ GeV}}{0.4 \text{ GeV}} \right), \quad (21)$$

$$\beta_\lambda = 0.000103 + 0.000069 \left(\frac{M_t - 173.3 \text{ GeV}}{2.8 \text{ GeV}} \right) + 0.000028 \left(\frac{M_t - 173.3 \text{ GeV}}{2.8 \text{ GeV}} \right)^2 - 0.000013 \left(\frac{M_H - 125.6 \text{ GeV}}{0.4 \text{ GeV}} \right), \quad (22)$$

where the dependence of β_λ on $\alpha_s(M_Z)$ is of $O(10^{-7})$ and is not shown.

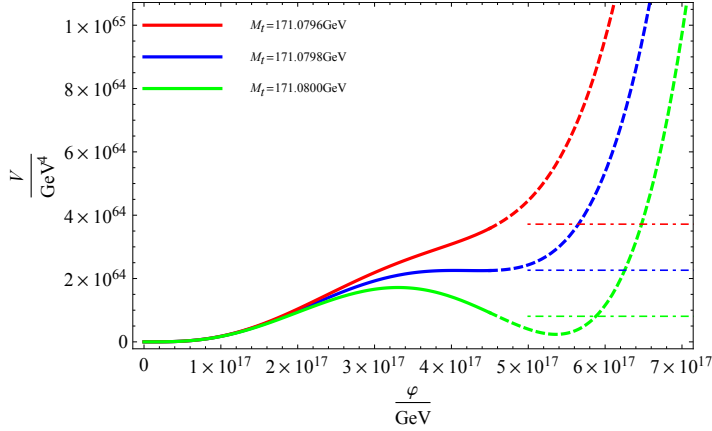


Figure 2: RGE improved Higgs potential (23), with $M_H = 125.6 \text{ GeV}$ and $\alpha_s = 0.1184$. The Solid and dashed lines are the SM Higgs potential (23). Beyond the UV cutoff Λ , which we have taken in this figure to be $4.5 \times 10^{17} \text{ GeV}$ as an illustration, we assume that the potential becomes flat as depicted by the dot-dashed lines.

3.3 Higgs inflation?

We have seen in Fig. 1 that both the Higgs self coupling λ and its beta function β_λ become very small at high scales $\mu \gtrsim 10^{17} \text{ GeV}$. This fact suggests that the SM Higgs field could be identified as an inflaton. In the following, we show that the SM Higgs potential becomes flat around 10^{17} GeV if we tune the top quark mass. However, we will see that it is difficult to reconcile this potential with the cosmological observation [60, 23].

For a field value $V = 246.22 \text{ GeV} \ll \varphi < \Lambda$, the Higgs potential becomes, with RGE improvement,

$$\mathcal{V}_{\text{SM}}(\varphi) = \frac{\lambda(\varphi)}{4} \varphi^4. \quad (23)$$

Around the scale 10^{17} GeV , this potential strongly depends on the top quark mass, which we show by the solid and dashed lines in Fig. 2. The dot-dashed lines are irrelevant to the argument of this subsection.

If we fine tune the top mass, we can have a saddle point in the Higgs potential: $\mathcal{V}_\varphi(\varphi) = \mathcal{V}_{\varphi\varphi}(\varphi) = 0$, as indicated by the middle (blue) line in Fig. 2. When we slightly lower the top mass, the saddle point disappears and the potential becomes monotonically increasing, as the upper (red) line. On the contrary, when we slightly raise the top mass, there appears another minimum at a high scale, as the lower (green) line [61, 62].

The middle (blue) line case, $M_t = 171.0798 \text{ GeV}$, gives the potential

$$\mathcal{V}_c = 6.0 \times 10^{-10} M_P^4 \sim (10^{16} \text{ GeV})^4 \quad (24)$$

⁷ In this definition, the graviton fluctuation $h_{\mu\nu}$ around the flat Minkowski spacetime: $g_{\mu\nu} = \eta_{\mu\nu} + 2M_P^{-1} h_{\mu\nu}$ becomes canonically normalized.

at the saddle point $\varphi_c = 4.2 \times 10^{17}$ GeV. One might think of using this saddle point for a Higgs inflation, but it is impossible due to the following reasons: With Eq. (8), this height of potential necessitates $\epsilon_V \sim 10^{-3}$. However, the point of $N_* \gtrsim 50$ becomes too close to the saddle point and gives $\epsilon_V \ll 10^{-3}$.

In order to avoid this problem, one might try lowering the top mass slightly to reproduce the value of $\epsilon_V \sim 10^{-3}$ at the inflection point $\mathcal{V}_{\varphi\varphi} = 0$. This still does not work because we cannot have enough e -foldings, $N_* \gtrsim 50$, at the inflection point.

As the third trial, one might choose ϵ_V freely at the inflection point so that one can have enough e -folding in passing the inflection point. In this case, one tries to reproduce $\epsilon_V \sim 10^{-3}$ at the higher point with $N_* \sim 50$. However, η_V at this point turns out to be too large to satisfy the slow-roll condition.

We present more detailed discussion in Appendix A.

Note that the precise value of M_t to give the saddle point in Fig. 2 depends on M_H , the details of the RGEs, etc.; the digits of M_t should not be taken literally, but be regarded as an indication how finely M_t must be tuned to yield a saddle point in the SM. Also the height of the potential at the saddle point varies when we change e.g. M_H within the 95% CL, $M_H = (124.8 - 126.4)$ GeV, as

$$\mathcal{V}_c = (1.5 - 32.) \times 10^{-10} M_P^4. \quad (25)$$

Therefore the value (24) should be taken as an indication of the order of magnitude.

4 Minimal Higgs inflation

We pursue the possibility that the Higgs potential above Λ becomes sufficiently flat to realize a viable inflation, as the dot-dashed lines in Fig. 2. The inflaton potential is bounded from above as in Eq. (8). In order to avoid the graceful exit problem, the Higgs potential must be monotonically increasing in all the range below and above Λ . Therefore, even if we allow an arbitrary modification above Λ , we still can get a bound: $\Lambda < 5 \times 10^{17}$ GeV. As a concrete example of the modification above Λ , we propose a log type potential and study its cosmological implications.

4.1 Constraint on top mass from minimal Higgs inflation

We have seen that the scale 10^{17} GeV gives the vanishing beta function β_λ . This scale is close to the string scale in the conventional perturbative superstring theory. Above the string scale, a conventional local field theory is altered. We have shown that the bare Higgs mass becomes very small around this scale [4]. This fact strongly suggests that the Higgs boson is a zero mass state of string theory. If it is the case, after integrating out all the massive stringy states, we get the effective potential, which is meaningful for field values beyond the string scale. The resultant potential beyond the string scale would be greatly modified from that in the SM.⁸

⁸ On the contrary, if the Higgs boson had a string-scale bare mass, it would come from a string massive mode. Then considering the effective potential would become meaningless, as it would become one of the fields

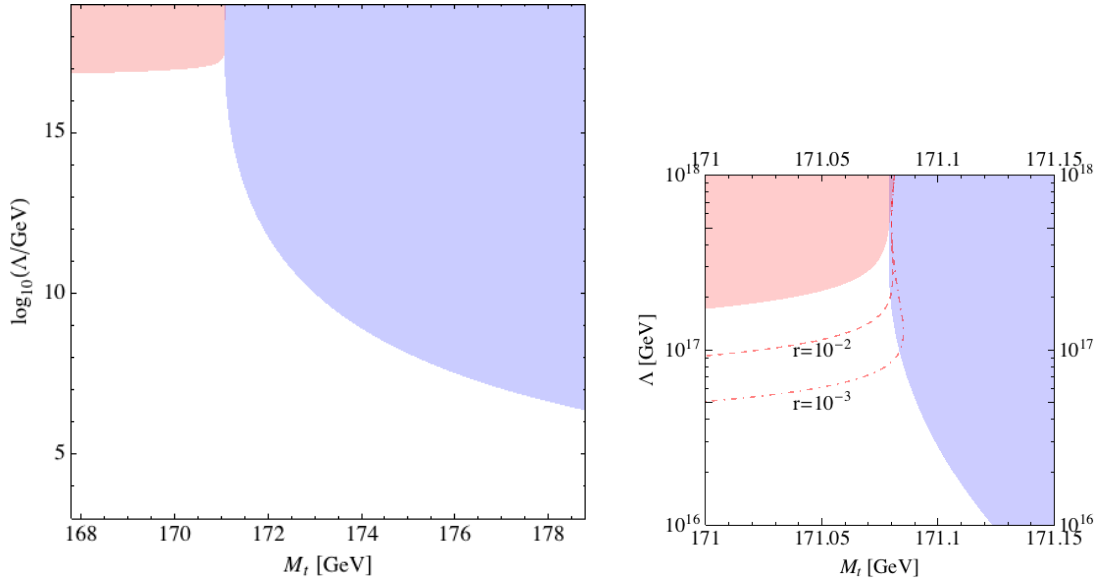


Figure 3: Left: Excluded region by Eq. (27) (red, left) and by Eq. (26) (blue, right) in $\log_{10}(\Lambda/\text{GeV})$ vs M_t plane. Right: Enlarged view for Λ vs M_t . Expected future exclusion limits within 95%CL: $r < 10^{-2}$ and 10^{-3} are also presented by dashed and dot-dashed lines, respectively.

As we have discussed in Introduction, it is plausible that the effective potential for the field value beyond Λ becomes almost flat. This opens up a possibility that this flat potential can be used for the inflation. Firstly in this subsection, we consider a necessary condition for the SM potential at $\varphi < \Lambda$ to allow such a modification in the region $\varphi > \Lambda$.

To avoid the graceful exit problem [39, 40, 41], the Higgs potential must be a monotonically increasing function of φ in all the range below and above Λ .⁹ Therefore, we have

$$\frac{d\mathcal{V}_{\text{SM}}}{d\varphi} = \frac{1}{4}(\beta_\lambda + 4\lambda)\varphi^3 > 0, \quad (26)$$

for all the scales below the cutoff: $\varphi < \Lambda$, and the upper bound (13) leads to

$$\mathcal{V}_{\text{SM}}(\Lambda) < \mathcal{V}_{\text{max}}. \quad (27)$$

We show excluded regions on the Λ - M_t plane from the above two constraints in the left panel of Fig. 3. The left (red) region is excluded by the condition (27) within 95% CL and the right (blue) region is forbidden by Eq. (26). The right panel is an enlarged view. The dashed and dot-dashed lines correspond to the

to be integrated out.

⁹ If there is a potential barrier, then the phase transition becomes first order. This is problematic: The false vacuum decays only through the tunneling. The bubbles of true vacuum expand with speed of light in the exponentially expanding medium of the false vacuum. They can hardly collide each other. See also Ref. [9] for a possible false vacuum inflation assuming a lowered Planck scale, which we do not employ in this paper.

exclusion limits at the 95% CL, $r < 10^{-2}$ and 10^{-3} , that are expected from the future experiments EPIC [63] and COre [64], respectively.

We see that the top quark mass needs to be $M_t \lesssim 171$ GeV if we want to have the cutoff scale to be at the string scale $\Lambda \sim 10^{17}$ GeV. If the top quark mass turns out to be heavier, say $M_t \gtrsim 173$ GeV, then this minimal scenario breaks down. However, it is possible that there exists an extra gauge-singlet scalar X that couples to the SM Higgs boson e.g. as

$$\mathcal{L} = -\frac{\rho}{4!}X^4 - \frac{\kappa}{2}\phi^\dagger\phi X^2, \quad (28)$$

where ρ and κ are coupling constants. Then X contributes to the running of λ positively, and the vacuum stability condition becomes milder. Such a scalar naturally arises in the Higgs portal dark matter scenario; see e.g. Refs. [65, 66, 67, 68, 69].¹⁰

4.2 Log type potential

So far we have not specified anything about the potential shape above Λ . In the following, let us examine the log-type potential:

$$\mathcal{V}(\varphi) = \mathcal{V}_1 \left(C + \ln \frac{\varphi}{M_P} \right). \quad (29)$$

We note that the Coleman-Weinberg potential with an explicit momentum cutoff Λ leads to a log type potential; see Appendix B.¹¹ The potential (29) leads to the slow roll parameters

$$\begin{aligned} \epsilon_V &= \frac{1}{2} \left(\frac{M_P}{\varphi} \right)^2 \left(\frac{1}{C + \ln \frac{\varphi}{M_P}} \right)^2, & \eta_V &= - \left(\frac{M_P}{\varphi} \right)^2 \frac{1}{C + \ln \frac{\varphi}{M_P}}, \\ \xi_V^2 &= 2 \left(\frac{M_P}{\varphi} \right)^4 \left(\frac{1}{C + \ln \frac{\varphi}{M_P}} \right)^2, & \varpi_V^3 &= -6 \left(\frac{M_P}{\varphi} \right)^6 \left(\frac{1}{C + \ln \frac{\varphi}{M_P}} \right)^3. \end{aligned} \quad (30)$$

The end point of the inflation is determined from Eq. (4) for a given constant C :

$$\varphi_{\text{end}} = \begin{cases} \frac{M_P}{\sqrt{2}W(e^C/\sqrt{2})} & \text{for } 0 < C < 0.153, \\ \sqrt{\frac{2}{W(2e^{2C})}} M_P & \text{for } C > 0.153, \end{cases} \quad (31)$$

where W is the Lambert function defined by $z = W(z)e^{W(z)}$. Equivalently, the constant C is fixed as a function of φ_{end} :

$$C = \begin{cases} \frac{M_P}{\sqrt{2}\varphi_{\text{end}}} - \ln \frac{\varphi_{\text{end}}}{M_P} & \text{for } \varphi_{\text{end}} \geq \sqrt{2}M_P, \\ \left(\frac{M_P}{\varphi_{\text{end}}} \right)^2 - \ln \frac{\varphi_{\text{end}}}{M_P} & \text{for } \varphi_{\text{end}} \leq \sqrt{2}M_P. \end{cases} \quad (32)$$

¹⁰ No matter X is included or not, our scenario is not altered by the right-handed neutrinos if their Dirac Yukawa couplings are $\lesssim 0.1$.

¹¹ In terms of the parameters given there, $C = \frac{\nu_0}{\nu_1} + \ln \frac{M_P}{\Lambda}$.

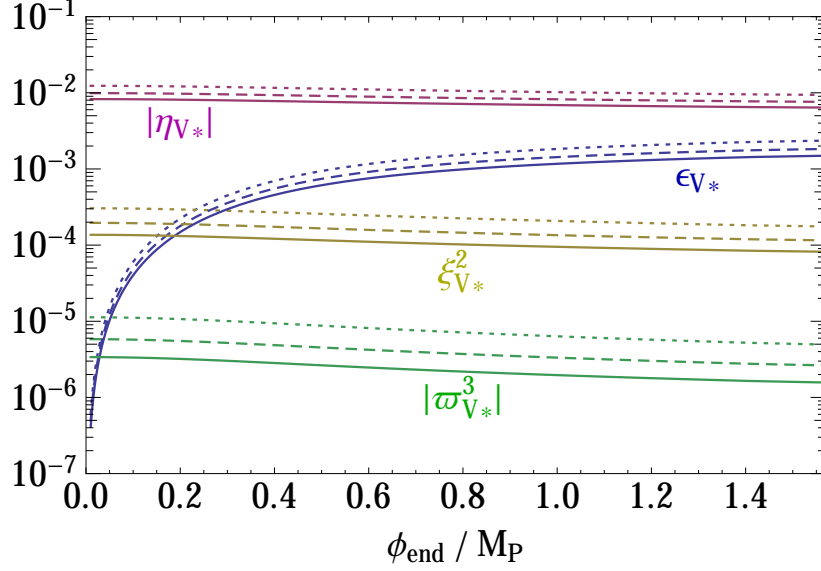


Figure 4: Slow roll parameters ϵ_{V*} , η_{V*} , ξ_{V*}^2 and ϖ_{V*}^3 as functions of φ_{end}/M_P within the range $0.01 < \varphi_{\text{end}}/M_P < 1.57$. The dotted, dashed, and solid lines correspond to $N_* = 40$, 50, and 60, respectively.

The e -folding becomes

$$\begin{aligned}
 N_* &= \frac{2C-1}{4} \frac{\varphi_*^2 - \varphi_{\text{end}}^2}{M_P^2} + \frac{\varphi_*^2}{2M_P^2} \ln \frac{\varphi_*}{M_P} - \frac{\varphi_{\text{end}}^2}{2M_P^2} \ln \frac{\varphi_{\text{end}}}{M_P} \\
 &= \frac{\varphi_*^2}{2M_P^2} \ln \frac{\varphi_*}{\varphi_{\text{end}}} - \frac{\varphi_*^2 - \varphi_{\text{end}}^2}{4M_P^2} \times \begin{cases} (1 - \sqrt{2}M_P/\varphi_{\text{end}}) & \text{for } \varphi_{\text{end}} \geq \sqrt{2}M_P, \\ (1 - 2M_P^2/\varphi_{\text{end}}^2) & \text{for } \varphi_{\text{end}} \leq \sqrt{2}M_P. \end{cases}
 \end{aligned} \tag{33}$$

To summarize: For a given φ_{end} , we fix the constant C by Eq. (32). Then we can obtain the slow roll parameters from Eq. (30) at any field value φ . The field value φ_* corresponding to a relevant e -folding N_* is determined from Eq. (33).

This way the slow roll parameters (30) at a given N_* is completely fixed. Note that they are independent of \mathcal{V}_1 , the overall normalization of the potential. In Fig. 4, we plot the slow roll parameters ϵ_V , η_V , ξ_V^2 , and ϖ_V^3 at the field value φ_* as functions of φ_{end}/M_P . The dotted, dashed and solid lines correspond to the values $N_* = 40$, 50 and 60, respectively.¹²

Once the slow roll parameters are given, the spectral indices, their running, and their running of running are completely fixed. In Fig. 5, we plot them as functions of φ_{end} . The solid (dotted) lines represent the values for N_* from 50 to 60 (40 to 49). The values for N_* below 50 are just for reference; e.g. the late time thermal inflation [70] can reduce the corresponding N_* to the observed value

¹² We have chosen the highest end point of the horizontal axis of Fig. 4 to be $\varphi_{\text{end}}/M_P = e^{W(1/\sqrt{2})} = 1.57$ at which $C = 0$ and $\mathcal{V}(\Lambda) = 0$. In this case, we cannot connect the potential \mathcal{V} to \mathcal{V}_{SM} , even if the latter were zero at Λ .

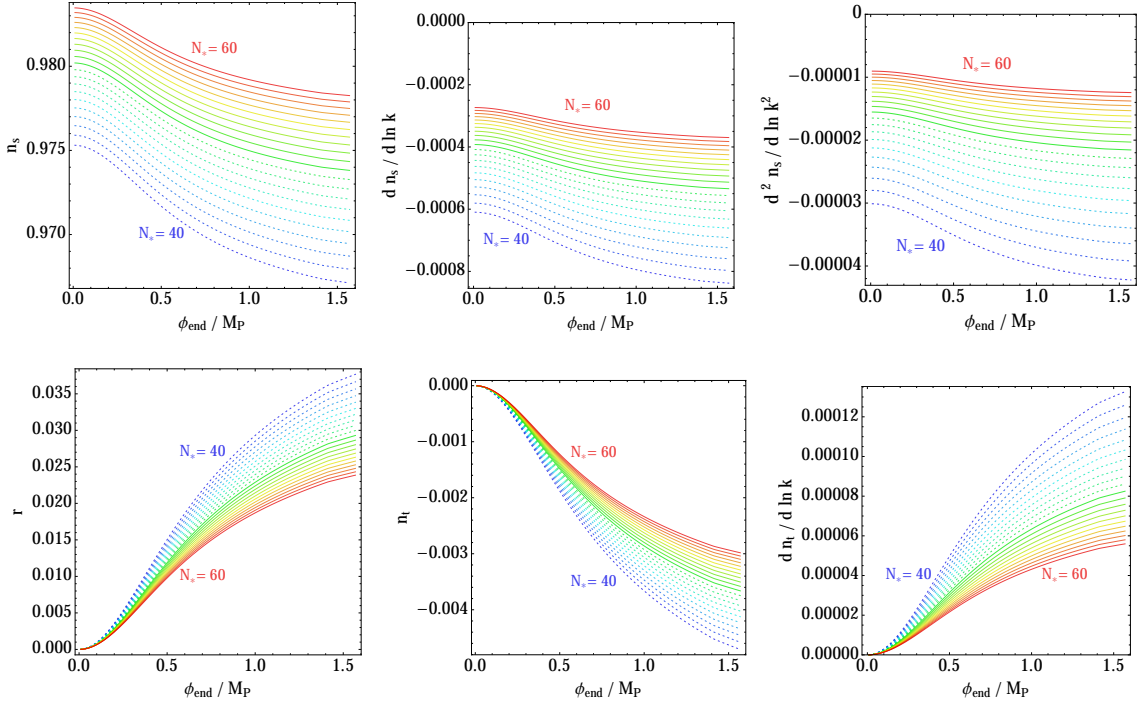


Figure 5: n_s , $\frac{dn_s}{d \ln k}$, $\frac{d^2 n_s}{d \ln k^2}$, r , n_t , and $\frac{dn_t}{d \ln k}$ as functions of φ_{end}/M_P .

of k_* ; see Ref. [71] for related discussions. When we vary N_* and φ_{end} within the ranges $50 \leq N_* \leq 60$ and $0 < \varphi_{\text{end}} < 1.57 M_P$, we get

$$\begin{aligned}
 0.980-0.984 > n_s > 0.974-0.979, & \quad 0 < r < 0.029-0.024, \\
 -(4.0-2.7) \times 10^{-4} > \frac{dn_s}{d \ln k} > -(5.3-3.7) \times 10^{-4}, & \quad 0 > n_t > -(3.7-3.0) \times 10^{-3}, \\
 -(1.6-0.9) \times 10^{-5} > \frac{d^2 n_s}{d \ln k^2} > -(2.2-1.2) \times 10^{-5}, & \quad 0 < \frac{dn_t}{d \ln k} < (8.2-5.6) \times 10^{-5},
 \end{aligned} \tag{34}$$

where the order of the inequality corresponds to that of $0 < \varphi_{\text{end}} < 1.57 M_P$; the range of numbers denoted by the en-dash “-” corresponds to the range $N_* = 50-60$.

So far we have not considered \mathcal{V}_1 , since it is sufficient to fix C to determine the slow-roll parameters. Now we determine \mathcal{V}_1 by the magnitude of the density perturbation (6):

$$\mathcal{V}_1 = 12\pi^2 A_s M_P^4 \left(\frac{M_P}{\varphi_*} \right)^2 \left(\frac{1}{C + \ln \frac{\varphi_*}{M_P}} \right)^3. \tag{35}$$

Then the potential and its derivatives at an e -folding N_* are completely fixed. In Fig. 6, we plot φ_* , \mathcal{V}_{end} , and \mathcal{V}_* as functions of φ_{end} . We indicate N_* the same as in Fig. 5.

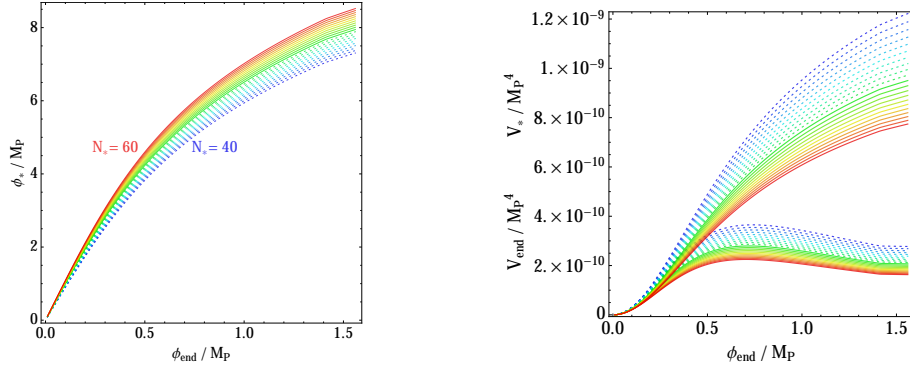


Figure 6: Left: φ_*/M_P as a function of φ_{end}/M_P . Right: Potential values, $\mathcal{V}_* = \mathcal{V}(\varphi_*)$ and $\mathcal{V}_{\text{end}} = \mathcal{V}(\varphi_{\text{end}})$, as functions of φ_{end}/M_P . The larger (smaller) values correspond to \mathcal{V}_*/M_P^4 ($\mathcal{V}_{\text{end}}/M_P^4$). We indicate N_* the same as in Fig. 5.

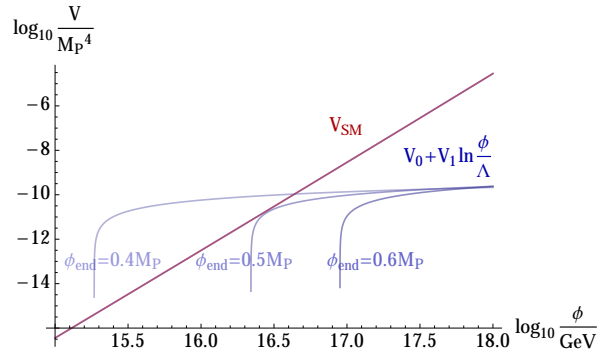


Figure 7: Three blue curves are high energy potential (58) for $\varphi_{\text{end}} = 0.4M_P$, $0.5M_P$, and $0.6M_P$ with $N_* = 50$. Red line is the SM potential (23) with the top quark mass $M_t = 170.5 \text{ GeV}$.

For a given φ_{end} we have obtained the constants \mathcal{V}_1 and C . If we demand that the high scale potential (58), fixed by these values, is directly connected with the SM potential at Λ , then we can fix Λ by

$$\mathcal{V}_1 \left(C + \ln \frac{\Lambda}{M_P} \right) = \mathcal{V}_{\text{SM}}(\Lambda). \quad (36)$$

In Fig. 7 we present left and right hand sides of Eq. (36) for $N_* = 50$ and $M_t = 170.5 \text{ GeV}$ to illustrate the situation. We see that the low energy SM potential can be directly connected to the high energy one when and only when $\varphi_{\text{end}} \lesssim 0.5M_P$. This critical value of φ_{end} is not sensitive to the choice of N_* and M_t .

Then we plot r vs n_s , r vs $\frac{dn_s}{d \ln k}$, $\frac{dn_s}{d \ln k}$ vs n_s , and $\frac{d^2 n_s}{d \ln k^2}$ vs $\frac{dn_s}{d \ln k}$ for $0 < \varphi_{\text{end}} < 0.5M_P$ in Fig. 8, which can be compared with Figs. 1–5 in Ref. [37]. When we

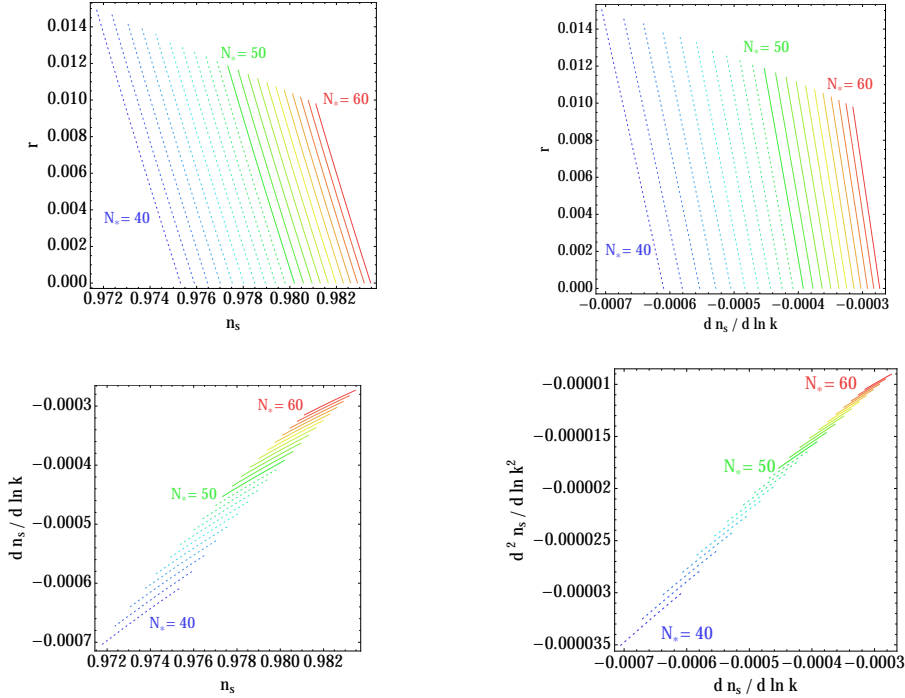


Figure 8: At upper-left, upper-right, lower-left, and lower-right, respectively, we have plotted r vs n_s , r vs $\frac{dn_s}{d \ln k}$, $\frac{dn_s}{d \ln k}$ vs n_s , and $\frac{d^2 n_s}{d \ln k^2}$ vs $\frac{dn_s}{d \ln k}$ for the potential (58) with $0 < \varphi_{\text{end}} < 0.5M_P$.

vary N_* and φ_{end} within the ranges $N_* = 50\text{--}60$ and $0 < \varphi_{\text{end}} < 0.5M_P$, we get

$$\begin{aligned}
0.980\text{--}0.983 > n_s > 0.977\text{--}0.981, & \quad 0 < r < 0.012\text{--}0.010, \\
-(3.9\text{--}2.7) \times 10^{-4} > \frac{dn_s}{d \ln k} > -(4.5\text{--}3.1) \times 10^{-4}, & \quad 0 > n_t > -(1.5\text{--}1.2) \times 10^{-3}, \\
-(1.6\text{--}0.9) \times 10^{-5} > \frac{d^2 n_s}{d \ln k^2} > -(1.8\text{--}1.0) \times 10^{-5}, & \quad 0 < \frac{dn_t}{d \ln k} < (3.1\text{--}2.2) \times 10^{-5},
\end{aligned} \tag{37}$$

where the order of the inequality corresponds to that of $0 < \varphi_{\text{end}} < 0.5M_P$; see Eq. (34). From Fig. 5, we see that we need rather small $N_* \sim 40$ for $0 < \varphi_{\text{end}} < 0.5M_P$ in order to account for the observed value of n_s in Eq. (10).

We note that a large field inflation with scale $\gtrsim 10^{17}$ GeV tends to require relatively high value of N_* , barring the late-time thermal inflation mentioned above. When we approximate that the Higgs field decays into the SM modes instantaneously after the inflation [42], the reheating temperature is given by¹³

$$\frac{\pi^2}{30} g_* T_{\text{reh}}^4 = \mathcal{V}_{\text{end}}, \tag{38}$$

¹³ We note that the scale φ_{end} is beyond Λ , which is the UV cutoff scale of the SM. Generically one expects that, above Λ , there appears extra degrees of freedom besides the SM modes. In general, these modes, say excited string modes in string theory, decay with the rate of the order of Λ times a coupling constant, and we assume that these modes in the decay chain does not affect the result very much.

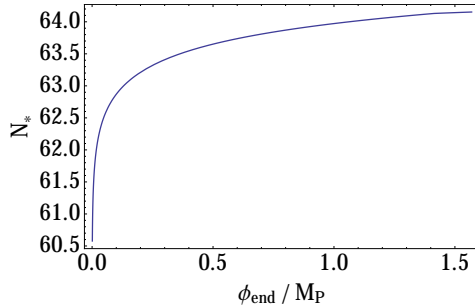


Figure 9: The e -foldings N_* as a function of φ_{end}/M_P corresponding to the pivot scale $k_* = 0.002 \text{ Mpc}^{-1}$ in the instantaneous decay approximation; see text.

where $g_* \simeq 106.75$ is the effective number of degrees of freedom in the SM; the resultant reheating temperature is $T_{\text{reh}} \simeq 4 \times 10^{15} \text{ GeV}$ for $\varphi_{\text{end}} = 0.5M_P$. Then the e -folding number, corresponding to the pivot scale $k_* = 0.002 \text{ Mpc}^{-1}$ and the Hubble parameter $H_0 = 67.3 \text{ km s}^{-1} \text{ Mpc}^{-1}$, is given by [37]:

$$N_* \simeq 69 + \frac{1}{4} \ln \frac{\mathcal{V}_*}{M_P^4} + \frac{1}{4} \ln \frac{\mathcal{V}_*}{\mathcal{V}_{\text{end}}}. \quad (39)$$

Using the value of \mathcal{V}_* and \mathcal{V}_{end} as depicted in Fig. 6, we get the e -folding number as a function of φ_{end} , which is plotted in Fig. 9. This indicates that the large field inflation requires $N_* \gtrsim 60$.

On the other hand, as we have seen around Eq. (36) and Eq. (37), we need a small value of $N_* \sim 40$, if we want to directly connect the log potential with the SM one. To do so, φ_{end} needs relatively small, $\varphi_{\text{end}} < 0.5M_P$, and N_* should be around 40 in order to obtain a realistic value of n_s .

There are two ways to solve this apparent inconsistency. One is to note that indeed we do not have to connect the log potential to \mathcal{V}_{SM} so strictly, as it is unclear what happens around $\varphi \sim \Lambda$.¹⁴ All we need is that the end point value of the inflaton potential is larger than the SM potential at its UV cutoff scale: $\mathcal{V}_{\text{end}} > \mathcal{V}_{\text{SM}}(\Lambda)$ for $\varphi_{\text{end}} > \Lambda$. Then we can take larger φ_{end} to obtain smaller value of n_s .

The other is adding a small correction to the log potential:

$$\Delta\mathcal{V} = \mathcal{V}_1 \left(c_1 \frac{\varphi}{M_P} + c_2 \frac{\varphi^2}{M_P^2} + \dots \right). \quad (40)$$

For example, if we choose $\mathcal{V}_1 = 4 \times 10^{-11} M_P^4$, $C = 5$, $c_1 = 0.1$, $c_2 = -0.01$, and $c_n = 0$ for $n \geq 3$, then we get $\varphi_{\text{end}} = 0.48 M_P$, $\varphi_* = 4.7 M_P$, $N_* = 64$, $r = 0.008$ and $n_s = 0.978$. The resultant potential is illustrated in Fig. 10.

¹⁴ For example, the Coleman-Weinberg potential that has an explicit momentum cutoff Λ turns into the log-type potential only at large field values $\varphi \gg \Lambda$ as shown in Appendix B.

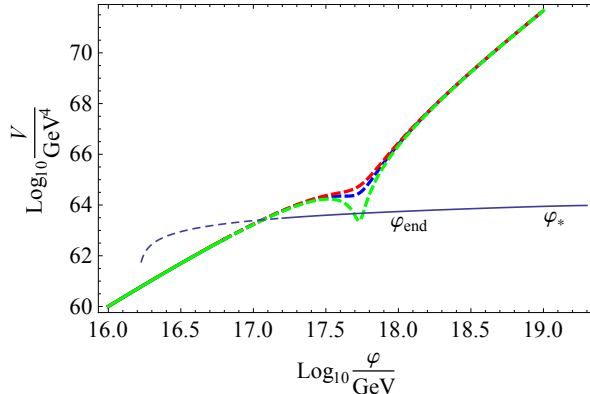


Figure 10: Log potential (29) plus the correction (40) as a function of φ is drawn in the log-log plot as the solid line in the right, which is the modification of the line for $\varphi_{\text{end}} = 0.5M_P$ in Fig. 7; φ_* and φ_{end} are also indicated. The SM lines are the same as in Fig. 2 but the SM cutoff is taken to be slightly smaller $\Lambda \simeq 10^{17}$ GeV.

5 Summary and discussions

The Higgs potential in the Standard Model (SM) can have a saddle point around 10^{17} GeV, and its height is suppressed because the Higgs quartic coupling becomes small. These facts suggest that the SM Higgs field may serve as an inflaton, without assuming the very large coupling to the Ricci scalar of order 10^4 , which is necessary in the ordinary Higgs inflation scenario. In this paper, we have pursued the possibility that the Higgs potential becomes almost flat above the UV cutoff Λ .

Since a first order phase transition at the end of the inflation leads to the graceful exit problem, the Higgs potential must be monotonically increasing in all the range below and above Λ . From this condition, we get an upper bound on Λ to be of the order of 10^{17} GeV.

We have briefly sketched the possible log type potential above Λ . We present the motivation of this shape in Appendix B, that is, the Coleman-Weinberg one-loop effective potential becomes of this type above Λ when the momentum integral is cut off by Λ . The predictions on the parameters of the cosmic microwave background at the e -foldings $N_* = 50$ – 60 are: the scalar spectral index, 0.980 – $0.983 > n_s > 0.977$ – 0.981 ; the tensor to scalar ratio, $0 < r < 0.012$ – 0.010 ; the running scalar index, $-(4.5$ – $3.1) \times 10^{-4} < dn_s/d \ln k < -(3.9$ – $2.7) \times 10^{-4}$; the running of running scalar index, $-(1.6$ – $0.9) \times 10^{-5} > d^2 n_s/d \ln k^2 > -(1.8$ – $1.0) \times 10^{-5}$; the tensor spectral index, $0 > n_t > -(1.5$ – $1.2) \times 10^{-3}$; and the running tensor index, $0 < dn_t/d \ln k < (3.1$ – $2.2) \times 10^{-5}$.

In this paper, we have pursued the bottom-up approach from the latest Higgs data, without assuming any other structure than the SM below Λ . We have shown in Fig. 3 that even if we allow arbitrary potential above Λ , still the restriction is rather severe to achieve this minimal Higgs inflation scenario.

It is curious that the upper bound on Λ from the minimal Higgs inflation coincides with the scale where the quartic coupling λ and its beta function (and possibly the bare Higgs mass) vanish. This coincident scale $\sim 10^{17}$ GeV is close

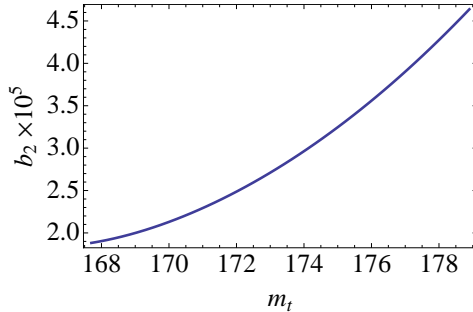


Figure 11: Running of the beta function b_2 at the scale Λ_0 of vanishing beta function as a function of top pole mass M_t .

to the string scale in the conventional perturbative superstring scenario.¹⁵ This fact may suggest that the physics of the SM, string theory, and the universe are all directly connected.

There are possibilities that realizes the flatness from the gauge symmetry as in the gauge-Higgs unification scenario [31, 32, 33, 34, 35]. See also Refs. [29, 30] for other stringy attempts. Furthermore, Ref. [72, 73] derives the log potential of the type (58). It would be interesting to construct a realistic string model that breaks the supersymmetry at string scale¹⁶ and realizes the flat Higgs potential above Λ consistent to the cosmological observations. One can even go beyond the symmetry argument of the ordinary quantum field theory/string theory to realize the flat potential, such as with the MPP [21, 22, 23], the classical conformality around Λ [77, 24, 25, 26, 27], the multiverse [78], the anthropic principle [79], etc.

Acknowledgement

We thank Tetsutaro Higaki for a useful comment. We also thank Finelli Fabio for his kind explanation about Ref. [37]. This work is in part supported by the Grant-in-Aid for Scientific Research Nos. 22540277 (HK), 23104009, 20244028, and 23740192 (KO) and for the Global COE program “The Next Generation of Physics, Spun from Universality and Emergence.” The work of Y. H. was supported by a Grant-in-Aid for Japan Society for the Promotion of Science (JSPS) Fellows No.25-1107.

Appendix

A SM Higgs as inflaton

To see more explicitly the argument shown in Sec. 3.3 for the difficulty in directly using the SM Higgs field as an inflaton, we first show how to make a saddle point.

¹⁵ See e.g. Refs. [29, 30] for trials to explain the smallness of the quartic coupling in string theory context.

¹⁶ Generally number of superstring vacua that breaks supersymmetry at string scale is much larger than the one that preserves supersymmetry [74, 75, 76].

Let us expand the potential around the point φ_0 ($\sim 10^{17}$ GeV) of vanishing beta function $\beta_\lambda = 0$:

$$\mathcal{V}|_{\varphi \sim \varphi_0} = \frac{\varphi^4}{4} \left[\lambda_0 + b_2 \left(\ln \frac{\varphi}{\varphi_0} \right)^2 + b_3 \left(\ln \frac{\varphi}{\varphi_0} \right)^3 + \dots \right], \quad (41)$$

where b_i are given by

$$b_2 = \frac{1}{2} \frac{d^2 \lambda}{d \ln \mu^2} = \frac{1}{2} \sum_i \beta_i \frac{\partial \beta_\lambda}{\partial \lambda_i}, \quad b_n = \frac{1}{n!} \frac{d^n \lambda}{d \ln \mu^n} = O\left((16\pi^2)^{-n}\right), \quad (42)$$

with λ_i representing [4] the Yukawa coupling squared, y_t^2 etc., the gauge coupling squared, g_Y^2 , g_2^2 , g_3^2 , and the quartic coupling λ . Note that each $\beta_i = d\lambda_i/d \ln \mu$ has a loop suppression factor $1/16\pi^2$. We see that the SM Higgs potential can always have a saddle point by choosing a particular value of λ_0 by adjusting the top quark mass. For example, when we approximate $b_3 = 0$, the saddle point is realized at $\varphi = e^{-1/4} \varphi_0$ by choosing $\lambda_0 = b_2/16$. In the SM, b_2 takes values $b_2 \simeq (1.9-4.6) \times 10^{-5}$ for the 95% confidence interval from the top quark mass (15), see Fig. 11.

In order to show the difficulty of the inflection point inflation with the SM Higgs potential, it suffices to expand the potential around its inflection point φ_c that satisfies $\mathcal{V}_c'' := \mathcal{V}_{\varphi\varphi}(\varphi_c) = 0$:

$$\mathcal{V}(\varphi) = \mathcal{V}_c + \mathcal{V}_c' (\varphi - \varphi_c) + \frac{\mathcal{V}_c'''}{3!} (\varphi - \varphi_c)^3 + \dots, \quad (43)$$

where $\mathcal{V}_c''' := \mathcal{V}_{\varphi\varphi\varphi}(\varphi_c)$ and we tune the top quark mass in order to make $\mathcal{V}_c' := \mathcal{V}_\varphi(\varphi_c)$ very small. The e -folding from $\varphi_c + \delta\varphi_*$ to $\varphi_c - \delta\varphi_{\text{end}}$ becomes

$$\begin{aligned} N_* &= \sqrt{\frac{2}{\mathcal{V}_c' \mathcal{V}_c'''} M_P^2} \left[\arctan \left(\sqrt{\frac{\mathcal{V}_c'''}{2\mathcal{V}_c'}} \delta\varphi_{\text{end}} \right) + \arctan \left(\sqrt{\frac{\mathcal{V}_c'''}{2\mathcal{V}_c'}} \delta\varphi_* \right) \right] \\ &+ \frac{2\mathcal{V}_c'}{3M_P^2 \mathcal{V}_c'''} \ln \frac{2\mathcal{V}_c' + \mathcal{V}_c''' \delta\varphi_*^2}{2\mathcal{V}_c' + \mathcal{V}_c''' \delta\varphi_{\text{end}}^2} + \frac{\delta\varphi_*^2 - \delta\varphi_{\text{end}}^2}{6M_P^2}. \end{aligned} \quad (44)$$

In the following, we discuss in detail the three cases that are sketched in the text:

- First possibility is to put $\mathcal{V}_c' = 0$ and earn the e -folding near the saddle point. The e -folding (44) for $\delta\varphi_{\text{end}} > 0$ and $\delta\varphi_* < 0$ becomes

$$N_* = \frac{2\mathcal{V}_c}{M_P^2 \mathcal{V}_c'''} \left(\frac{1}{|\delta\varphi_*|} - \frac{1}{\delta\varphi_{\text{end}}} \right) - \frac{\delta\varphi_{\text{end}}^2 - \delta\varphi_*^2}{6M_P^2} \simeq \frac{2\mathcal{V}_c}{M_P^2 \mathcal{V}_c''' |\delta\varphi_*|}. \quad (45)$$

Close to the saddle point, we have

$$\epsilon_V = \frac{M_P^2 (\mathcal{V}_c''')^2}{8\mathcal{V}_c'^2} \delta\varphi_*^4 + O(\delta\varphi_*^7). \quad (46)$$

Putting Eq. (45) into Eq. (46), the slow roll parameter reads

$$\epsilon_V = \frac{2\mathcal{V}_c'^2}{N_*^4 M_P^6 (\mathcal{V}_c''')^2}, \quad (47)$$

and hence the scalar perturbation becomes

$$A_s = \frac{N_*^4 M_P^2 (\mathcal{V}_c''')^2}{48\pi^2 \mathcal{V}_c}. \quad (48)$$

From Eq. (41), we can compute the values in the SM:

$$\mathcal{V}_c''' \sim 10^{-5} \varphi_c \sim 10^{-6} M_P \quad (49)$$

which results in $A_s \gg 1$, far larger than the allowed value (8).

- As a second possibility, one might introduce small $\mathcal{V}_c' \sim 10^{-11} M_P^3$ at φ_c , in order to realize the value of the correct density perturbation at φ_c . For the SM values $\mathcal{V}_c \sim 10^{-9} M_P^4$ and $\mathcal{V}_c''' = 10^{-6} M_P$, we obtain from Eq. (44) the e -folding

$$N_* \sim 1. \quad (50)$$

This does not work.

- Finally one may take very tiny \mathcal{V}_c' at φ_c to earn enough e -folding, in order to realize the inflection point inflation scenario [80, 81, 82, 83, 84, 85, 86, 87, 88, 89], while obtaining necessary amount of ϵ_V at a point above the inflection point: $\varphi_c + \delta\varphi_*$ with $\delta\varphi_* > 0$. In passing through the inflection point φ_c from φ_* ($> \varphi_c$) to φ_{end} ($< \varphi_c$), we earn the e -folding

$$N_* = \sqrt{\frac{2\pi^2 \mathcal{V}_c^2}{M_P^4 \mathcal{V}_c' \mathcal{V}_c'''} + O((\mathcal{V}_c')^0)}, \quad (51)$$

and hence we can have as large an e -folding as we want by tuning \mathcal{V}_c' small. More concretely, we need

$$\mathcal{V}_c' \sim 10^{-15} M_P^3 \quad (52)$$

to get $N_* \sim 50$ with Eq. (49). However, to keep the slow roll parameter

$$\eta_V = \frac{M_P^2 \mathcal{V}_c'''}{\mathcal{V}_c} \delta\varphi_* + O(\delta\varphi_*^2) \quad (53)$$

sufficiently small, we need to be close to the inflection point:

$$\delta\varphi_* \ll \frac{\mathcal{V}_c}{M_P^2 \mathcal{V}_c'''} \quad (54)$$

Within this range, we get

$$\epsilon_V = \frac{\mathcal{V}_c^2 \eta_V^4}{8M_P^6 (\mathcal{V}_c''')^2} \ll \frac{\mathcal{V}_c^2}{8M_P^6 (\mathcal{V}_c''')^2}. \quad (55)$$

- When $\delta\varphi_*^2 \gg 2\mathcal{V}_c'/\mathcal{V}_c'''$, we have the same expression as Eq. (46). From Eq. (55), we get

$$A_s = \frac{\mathcal{V}_c}{24\pi^2 M_P^4 \epsilon_V} \gg \frac{M_P^2 (\mathcal{V}_c''')^2}{3\pi^2 \mathcal{V}_c}. \quad (56)$$

Putting the SM values, this results in $A_s \gg 10^{-5}$ which is far larger than the observation (8).

- On the contrary when $\delta\varphi_*^2 \ll 2\mathcal{V}'_c/\mathcal{V}'''_c$, we get $\epsilon_V = M_P^2 (\mathcal{V}'_c)^2 / 2\mathcal{V}_c^2$ and hence

$$A_s = \frac{\mathcal{V}_c^3}{12\pi^2 M_P^6 (\mathcal{V}'_c)^2} \sim 1, \quad (57)$$

where we have put Eq. (52). We see that this is too large again.

B Motivating log type toy model

We present a motivation for the toy model with the log type potential at $\varphi > \Lambda$:

$$\mathcal{V} = \mathcal{V}_0 + \mathcal{V}_1 \ln \frac{\varphi}{\Lambda} =: \tilde{\mathcal{V}}_0 + \mathcal{V}_1 \ln \frac{\varphi}{M_P}. \quad (58)$$

In the bare perturbation theory, see e.g. Ref. [4], the one-loop effective potential for the Higgs field φ is given by

$$\mathcal{V}_{\text{eff}}(\varphi) = \frac{m_B^2}{2}\varphi^2 + \frac{\lambda_B}{4}\varphi^4 + \sum_i \frac{N_i}{2} \int \frac{d^4 p}{(2\pi)^4} \ln \frac{p^2 + c_i \varphi^2}{p^2}, \quad (59)$$

where the integration is performed over Euclidean four momentum.¹⁷ Since we are interested in the behavior of the potential at the field value φ very much larger than the electroweak scale $\varphi \gg V = 246.22 \text{ GeV}$, we work in the symmetric phase by setting the Higgs VEV to be zero: $V = 0$. The number of degrees of freedom, N_i , and the coupling to the Higgs, c_i , are summarized in Table 1 for species i that have non-negligible coupling to the Higgs. h and χ are the physical and Nambu-Goldstone modes of the Higgs around the field value φ , respectively.¹⁸ Assuming existence of an underlying gauge invariant regularization, such as string theory, let us cutoff the integral by $|p| < \Lambda$:

$$\frac{d\mathcal{V}_{\text{eff}}}{d\varphi^2} = \frac{1}{2} \left[m_B^2 + \lambda_B \varphi^2 + \sum_i \frac{N_i c_i}{16\pi^2} \left(\Lambda^2 - c_i \varphi^2 \ln \frac{\Lambda^2 + c_i \varphi^2}{c_i \varphi^2} \right) \right]. \quad (60)$$

The bare Higgs mass m_B^2 is tuned to yield the desired value of the low energy mass-squared parameter,

$$m_R^2 := 2 \left. \frac{d\mathcal{V}_{\text{eff}}}{d\varphi^2} \right|_{\varphi^2 \rightarrow 0}, \quad (61)$$

to be zero: $m_R^2 = 0$, see e.g. Ref. [4].¹⁹ Then we get

$$m_B^2 = -\frac{\Lambda^2}{16\pi^2} \sum_i N_i c_i. \quad (62)$$

¹⁷ In Eq. (59), we have tuned the cosmological constant so that we get $\mathcal{V}_{\text{eff}} \rightarrow 0$ as $\varphi \rightarrow 0$.

¹⁸ Though we show our results in the Landau gauge, we can explicitly show that in the R_ξ gauge, depending on the external field φ , the one-loop result (59) is independent of the gauge parameter ξ if we expand it by $c_i \varphi^2 \ll \Lambda^2$.

¹⁹ Recall that we are working in the symmetric phase.

To summarize, we generally have

$$\frac{d\mathcal{V}_{\text{eff}}}{d\varphi^2} = \frac{\varphi^2}{2} \left[\lambda_B - \sum_i \frac{N_i c_i^2}{16\pi^2} \ln \frac{\Lambda^2 + c_i \varphi^2}{c_i \varphi^2} \right]. \quad (63)$$

We see that the bare mass drops out of the effective potential, as it should be. The form (63) corresponds to the one loop correction to λ_B . As a side remark, we comment that the condition $m_B^2 = 0$ at this one-loop order, namely $\sum_i N_i c_i = 0$, is the celebrated Veltman condition [90, 4].

Rigorously speaking, the effective potential (59) or (63) can be trusted only when the field dependent mass in the loop integral is sufficiently small: $c_i \varphi^2 \ll \Lambda^2$. Nonetheless, let us venture to assume that the expression (59) or (63) is still valid even for the field values much larger than the cutoff Λ .²⁰ When we can take $c_j \varphi^2 \gg \Lambda^2$ for some species j , say $j = W, Z, t$, and $c_i \varphi^2 \ll \Lambda^2$ for others i , then

$$\frac{d\mathcal{V}_{\text{eff}}}{d\varphi^2} \rightarrow \frac{1}{2} \left[m_B^2 + \lambda_B^2 \varphi^2 + \frac{\Lambda^4}{16\pi^2 \varphi^2} \sum_{j: c_j \varphi^2 \gg \Lambda^2} \frac{N_j}{2} \right]. \quad (64)$$

We note that the bare mass re-appears in this limit. As one can see from Fig. 1, both the bare coupling λ_B , approximated by the $\overline{\text{MS}}$ one $\lambda(\Lambda)$, and the bare mass m_B^2 are very close to zero for $\Lambda \gtrsim 10^{17}$ GeV. If the UV theory somehow chooses the bare mass to be zero, as is proposed by Veltman, and also $\lambda_B = 0$, then the effective potential becomes

$$\mathcal{V}_{\text{eff}} \rightarrow \mathcal{V}_0 + \frac{\Lambda^4}{16\pi^2} \ln \frac{\varphi}{\Lambda} \sum_{j: c_j \varphi^2 \gg \Lambda^2} \frac{N_j}{2} \quad (65)$$

at $c_j \varphi^2 \gg \Lambda^2$, where \mathcal{V}_0 is an integration constant. We see that the potential at very high scales takes the form of Eq. (58).

We can read off the coefficient \mathcal{V}_1 in Eq. (58) from Eq. (65):

$$\mathcal{V}_1 = -\frac{3}{32\pi^2} \Lambda^4 \quad (66)$$

when we put $j = W, Z, t$. We see that we need to add extra scalar fields coupling to the Higgs to make \mathcal{V}_1 positive at high scales, as in the Higgs portal dark matter scenario. As an illustration, we assume hereafter that the Higgs potential is not modified up to the cutoff Λ and is connected to Eq. (58) directly at Λ with arbitrary constants \mathcal{V}_0 and \mathcal{V}_1 , though generally the RGE itself can be changed by the inclusion of the extra scalar fields.

C Limiting behavior

We show the limiting behavior of the high energy potential Eq. (58).

²⁰ As is suggested in Ref. [91], the number of the effective degrees of freedom may be greatly reduced above the string scale. If this is the case, the naive cutoff removing the modes $|p| > \Lambda$ might be a good illustration of the correct picture.

i	h	χ	W	Z	t
N_i	1	3	6	3	$-4N_c$
c_i	$3\lambda_B$	λ_B	$g_{2B}^2/4$	$(g_{2B}^2 + g_{YB}^2)/4$	$y_{tB}^2/2$

Table 1: Constants given in Eq. (59) for species i providing large c_i .

- In the limit $\mathcal{V}_1 \ll \tilde{\mathcal{V}}_0$, we get $\tilde{\mathcal{V}}_0 \rightarrow \mathcal{V}_0$,

$$\begin{aligned} \epsilon_V &\rightarrow \frac{1}{2} \left(\frac{M_P}{\varphi} \right)^2 \left(\frac{\mathcal{V}_1}{\mathcal{V}_0} \right)^2, & \eta_V &\rightarrow - \left(\frac{M_P}{\varphi} \right)^2 \frac{\mathcal{V}_1}{\mathcal{V}_0}, \\ \xi_V^2 &\rightarrow 2 \left(\frac{M_P}{\varphi} \right)^4 \left(\frac{\mathcal{V}_1}{\mathcal{V}_0} \right)^2, & \varpi_V^3 &\rightarrow -6 \left(\frac{M_P}{\varphi} \right)^6 \left(\frac{\mathcal{V}_1}{\mathcal{V}_0} \right)^3, \end{aligned} \quad (67)$$

and hence

$$\frac{\varphi_{\text{end}}}{M_P} \rightarrow \sqrt{\frac{\mathcal{V}_1}{\mathcal{V}_0}} \ll 1, \quad N_* \rightarrow \frac{\mathcal{V}_0}{2\mathcal{V}_1} \left(\frac{\varphi_*}{M_P} \right)^2, \quad n_s \rightarrow 1 - \frac{1}{N_*}, \quad r \rightarrow \frac{4\mathcal{V}_1}{N_*\mathcal{V}_0}. \quad (68)$$

For an observed value of A_s , we get

$$\frac{\mathcal{V}_0}{M_P^4} = \sqrt{\frac{6\pi^2 A_s \mathcal{V}_1}{N_* M_P^4}}. \quad (69)$$

Or if we remove $\mathcal{V}_1 = \mathcal{V}_0 \varphi_*^2 / 2N_* M_P^2$,

$$\frac{\mathcal{V}_0}{M_P^4} = \frac{3\pi^2 A_s}{N_*^2} \frac{\varphi_*^2}{M_P^2}. \quad (70)$$

Or else, we can rewrite $\mathcal{V}_1 = \left(\frac{\varphi_{\text{end}}}{M_P} \right)^2 \mathcal{V}_0$ to yield

$$\mathcal{V}_0 = \frac{6\pi^2 A_s}{N_*} \varphi_{\text{end}}^2 M_P^2, \quad \mathcal{V}_1 = \frac{6\pi^2 A_s}{N_*} \varphi_{\text{end}}^4, \quad \varphi_* = \sqrt{2N_*} \varphi_{\text{end}}. \quad (71)$$

- In the opposite limit $\tilde{\mathcal{V}}_0 \ll \mathcal{V}_1$, we get

$$\begin{aligned} \epsilon_V &\rightarrow \frac{1}{2} \left(\frac{M_P}{\varphi} \right)^2 \left(\frac{1}{\ln \frac{\varphi}{M_P}} \right)^2, & \eta_V &= - \left(\frac{M_P}{\varphi} \right)^2 \frac{1}{\ln \frac{\varphi}{M_P}}, \\ \xi_V^2 &= 2 \left(\frac{M_P}{\varphi} \right)^4 \left(\frac{1}{\ln \frac{\varphi}{M_P}} \right)^2, & \varpi_V^3 &= -6 \left(\frac{M_P}{\varphi} \right)^6 \left(\frac{1}{\ln \frac{\varphi}{M_P}} \right)^3. \end{aligned} \quad (72)$$

We define the end point of the inflation by the condition: $\max\{\epsilon_V, |\eta_V|\} = \epsilon_V = 1$, to get:

$$\varphi_{\text{end}} = e^{W(1/\sqrt{2})} M_P = 1.57 M_P. \quad (73)$$

Then the e -folding number becomes

$$N_* \rightarrow -\frac{\varphi_*^2 - \varphi_{\text{end}}^2}{M_P^2} + \frac{\varphi_*^2}{2M_P^2} \ln \frac{\varphi_*}{M_P} - \frac{\varphi_{\text{end}}^2}{2M_P^2} \ln \frac{\varphi_{\text{end}}}{M_P}, \quad (74)$$

which gives $\varphi_* = 8.54M_P$ ($7.96M_P$) for $N_* = 60$ (50), and hence

$$n_s \rightarrow 0.994 \quad (0.993), \quad r \rightarrow 6.2 \times 10^{-3} \quad (7.2 \times 10^{-3}). \quad (75)$$

This limit $\tilde{\mathcal{V}}_0 \ll \mathcal{V}_1$ gives the log-only potential. Note that

$$\mathcal{V}_{\text{end}} = W(1/\sqrt{2}) \mathcal{V}_1 = 0.45 \mathcal{V}_1. \quad (76)$$

We also get

$$\mathcal{V}_* = \mathcal{V}_1 \ln \frac{\varphi_*}{M_P} = 24\pi^2 A_s \epsilon_V M_P^4, \quad (77)$$

which gives $\mathcal{V}_1 = 1.23 \times 10^{-9} M_P^4$ ($1.46 \times 10^{-9} M_P^4$) and $\mathcal{V}_{\text{end}} = 3.23 \times 10^{-9} M_P^4$ ($3.75 \times 10^{-9} M_P^4$) for $N_* = 60$ (50).

References

- [1] ATLAS Collaboration, G. Aad et al., *Observation of a new particle in the search for the Standard Model Higgs boson with the ATLAS detector at the LHC*, Phys.Lett. **B716** (2012), 1–29, 1207.7214.
- [2] CMS Collaboration, S. Chatrchyan et al., *Observation of a new boson at a mass of 125 GeV with the CMS experiment at the LHC*, Phys.Lett. **B716** (2012), 30–61, 1207.7235.
- [3] P. P. Giardino, K. Kannike, I. Masina, M. Raidal, and A. Strumia, *The universal Higgs fit*, (2013), 1303.3570.
- [4] Y. Hamada, H. Kawai, and K.-y. Oda, *Bare Higgs mass at Planck scale*, Phys. Rev. D 87, **053009** (2013), 1210.2538.
- [5] M. Holthausen, K. S. Lim, and M. Lindner, *Planck scale Boundary Conditions and the Higgs Mass*, JHEP **1202** (2012), 037, 1112.2415.
- [6] F. Bezrukov, M. Y. Kalmykov, B. A. Kniehl, and M. Shaposhnikov, *Higgs Boson Mass and New Physics*, JHEP **1210** (2012), 140, 1205.2893.
- [7] G. Degrassi, S. Di Vita, J. Elias-Miro, J. R. Espinosa, G. F. Giudice, et al., *Higgs mass and vacuum stability in the Standard Model at NNLO*, JHEP **1208** (2012), 098, 1205.6497.
- [8] S. Alekhin, A. Djouadi, and S. Moch, *The top quark and Higgs boson masses and the stability of the electroweak vacuum*, Phys.Lett. **B716** (2012), 214–219, 1207.0980.
- [9] I. Masina, *The Higgs boson and Top quark masses as tests of Electroweak Vacuum Stability*, Phys.Rev. **D87** (2013), 053001, 1209.0393.
- [10] F. Jegerlehner, *The Standard model as a low-energy effective theory: what is triggering the Higgs mechanism?*, (2013), 1304.7813.

- [11] D. Buttazzo, G. Degrassi, P. P. Giardino, G. F. Giudice, F. Sala, et al., *Investigating the near-criticality of the Higgs boson*, (2013), 1307.3536.
- [12] F. Jegerlehner, *The hierarchy problem of the electroweak Standard Model revisited*, (2013), 1305.6652.
- [13] J. Sola, *Cosmological constant and vacuum energy: old and new ideas*, (2013), 1306.1527.
- [14] I. Masina and M. Quiros, *On the Veltman Condition, the Hierarchy Problem and High-Scale Supersymmetry*, (2013), 1308.1242.
- [15] M. Al-sarhi, I. Jack, and D. Jones, *Quadratic divergences in gauge theories*, Z.Phys. **C55** (1992), 283–288.
- [16] M. Einhorn and D. Jones, *The Effective potential and quadratic divergences*, Phys.Rev. **D46** (1992), 5206–5208.
- [17] C. F. Kolda and H. Murayama, *The Higgs mass and new physics scales in the minimal standard model*, JHEP **0007** (2000), 035, hep-ph/0003170.
- [18] J. Casas, J. Espinosa, and I. Hidalgo, *Implications for new physics from fine-tuning arguments. 1. Application to SUSY and seesaw cases*, JHEP **0411** (2004), 057, hep-ph/0410298.
- [19] D. Jones, *The quadratic divergence in the Higgs mass revisited*, Phys.Rev. **D88** (2013), 098301, 1309.7335.
- [20] CDF Collaboration, F. Abe et al., *Evidence for top quark production in $\bar{p}p$ collisions at $\sqrt{s} = 1.8$ TeV*, Phys.Rev.Lett. **73** (1994), 225–231, hep-ex/9405005.
- [21] C. Froggatt and H. B. Nielsen, *Standard model criticality prediction: Top mass 173 ± 5 -GeV and Higgs mass 135 ± 9 -GeV*, Phys.Lett. **B368** (1996), 96–102, hep-ph/9511371.
- [22] C. Froggatt, H. B. Nielsen, and Y. Takahashi, *Standard model Higgs boson mass from borderline metastability of the vacuum*, Phys.Rev. **D64** (2001), 113014, hep-ph/0104161.
- [23] H. B. Nielsen, *PREDICTED the Higgs Mass*, (2012), 94–126, 1212.5716.
- [24] S. Iso, N. Okada, and Y. Orikasa, *Classically conformal $B-L$ extended Standard Model*, Phys.Lett. **B676** (2009), 81–87, 0902.4050.
- [25] S. Iso, N. Okada, and Y. Orikasa, *The minimal $B-L$ model naturally realized at TeV scale*, Phys.Rev. **D80** (2009), 115007, 0909.0128.
- [26] M. Holthausen, M. Lindner, and M. A. Schmidt, *Radiative Symmetry Breaking of the Minimal Left-Right Symmetric Model*, Phys.Rev. **D82** (2010), 055002, 0911.0710.
- [27] S. Iso and Y. Orikasa, *TeV Scale $B-L$ model with a flat Higgs potential at the Planck scale - in view of the hierarchy problem -*, PTEP **2013** (2013), 023B08, 1210.2848.
- [28] Y. Hosotani, *Dynamical Mass Generation by Compact Extra Dimensions*, Phys.Lett. **B126** (1983), 309.

- [29] A. Hebecker, A. K. Knochel, and T. Weigand, *A Shift Symmetry in the Higgs Sector: Experimental Hints and Stringy Realizations*, JHEP **1206** (2012), 093, 1204.2551.
- [30] A. Hebecker, A. K. Knochel, and T. Weigand, *The Higgs mass from a String-Theoretic Perspective*, Nucl.Phys. **B874** (2013), 1–35, 1304.2767.
- [31] N. Haba, S. Matsumoto, N. Okada, and T. Yamashita, *Effective theoretical approach of Gauge-Higgs unification model and its phenomenological applications*, JHEP **0602** (2006), 073, hep-ph/0511046.
- [32] N. Haba, S. Matsumoto, N. Okada, and T. Yamashita, *Effective Potential of Higgs Field in Warped Gauge-Higgs Unification*, Prog.Theor.Phys. **120** (2008), 77–98, 0802.3431.
- [33] N. Maru and N. Okada, *Diphoton Decay Excess and 125 GeV Higgs Boson in Gauge-Higgs Unification*, Phys.Rev. **D87** (2013), 095019, 1303.5810.
- [34] N. Maru and N. Okada, *H to Z gamma in Gauge-Higgs Unification*, Phys.Rev. **D88** (2013), 037701, 1307.0291.
- [35] N. Maru and N. Okada, *Diphoton and Z photon Decays of Higgs Boson in Gauge-Higgs Unification: A Snowmass white paper*, (2013), 1307.8181.
- [36] S. R. Coleman and E. J. Weinberg, *Radiative Corrections as the Origin of Spontaneous Symmetry Breaking*, Phys.Rev. **D7** (1973), 1888–1910.
- [37] Planck Collaboration, P. Ade et al., *Planck 2013 results. XXII. Constraints on inflation*, (2013), 1303.5082.
- [38] J. Martin, C. Ringeval, and V. Vennin, *Encyclopaedia Inflationaris*, (2013), 1303.3787.
- [39] A. D. Linde, *A New Inflationary Universe Scenario: A Possible Solution of the Horizon, Flatness, Homogeneity, Isotropy and Primordial Monopole Problems*, Phys.Lett. **B108** (1982), 389–393.
- [40] S. Hawking, I. Moss, and J. Stewart, *Bubble Collisions in the Very Early Universe*, Phys.Rev. **D26** (1982), 2681.
- [41] A. H. Guth and E. J. Weinberg, *Could the Universe Have Recovered from a Slow First Order Phase Transition?*, Nucl.Phys. **B212** (1983), 321.
- [42] F. Bezrukov and M. Shaposhnikov, *The Standard Model Higgs boson as the inflaton*, Phys.Lett. **B659** (2008), 703–706, 0710.3755.
- [43] F. Bezrukov and M. Shaposhnikov, *Standard Model Higgs boson mass from inflation: Two loop analysis*, JHEP **0907** (2009), 089, 0904.1537.
- [44] F. Bezrukov, A. Magnin, M. Shaposhnikov, and S. Sibiryakov, *Higgs inflation: consistency and generalisations*, JHEP **1101** (2011), 016, 1008.5157.
- [45] A. Salvio, *Higgs Inflation at NNLO after the Boson Discovery*, (2013), 1308.2244.
- [46] J. Cervantes-Cota and H. Dehnen, *Induced gravity inflation in the SU(5) GUT*, Phys.Rev. **D51** (1995), 395–404, astro-ph/9412032.
- [47] J. Cervantes-Cota and H. Dehnen, *Induced gravity inflation in the standard model of particle physics*, Nucl.Phys. **B442** (1995), 391–412, astro-ph/9505069.

- [48] G. F. Giudice and H. M. Lee, *Unitarizing Higgs Inflation*, Phys.Lett. **B694** (2011), 294–300, 1010.1417.
- [49] H. M. Lee, *Running inflation with unitary Higgs*, Phys.Lett. **B722** (2013), 198–206, 1301.1787.
- [50] K. Kamada, T. Kobayashi, M. Yamaguchi, and J. Yokoyama, *Higgs G-inflation*, Phys.Rev. **D83** (2011), 083515, 1012.4238.
- [51] K. Kamada, T. Kobayashi, T. Takahashi, M. Yamaguchi, and J. Yokoyama, *Generalized Higgs inflation*, Phys.Rev. **D86** (2012), 023504, 1203.4059.
- [52] Tevatron Electroweak Working Group, D0 Collaborations, CDF, *Combination of CDF and DO results on the mass of the top quark using up to 8.7 fb⁻¹ at the Tevatron*, (2013), 1305.3929.
- [53] Y. Hamada, H. Kawai, and K.-y. Oda, *Bare Higgs mass and potential at ultraviolet cutoff*, (2013), 1305.7055.
- [54] F. Jegerlehner, M. Y. Kalmykov, and B. A. Kniehl, *About the EW contribution to the relation between pole and MS-masses of the top-quark in the Standard Model*, (2013), 1307.4226.
- [55] D0 Collaboration, V. M. Abazov et al., *Determination of the pole and MSbar masses of the top quark from the t \bar{t} cross section*, Phys.Lett. **B703** (2011), 422–427, 1104.2887.
- [56] CMS Collaboration, M. Aldaya, K. Lipka, and S. Naumann-Emme, *Determination of the top quark mass from the t \bar{t} cross section measured by CMS at $\sqrt{s} = 7$ TeV*, EPJ Web Conf. **28** (2012), 12044, 1201.5336.
- [57] R. Hempfling and B. A. Kniehl, *On the relation between the fermion pole mass and MS Yukawa coupling in the standard model*, Phys.Rev. **D51** (1995), 1386–1394, hep-ph/9408313.
- [58] F. Jegerlehner, M. Y. Kalmykov, and B. A. Kniehl, *On the difference between the pole and the MSbar masses of the top quark at the electroweak scale*, Phys.Lett. **B722** (2013), 123–129, 1212.4319.
- [59] Particle Data Group, J. Beringer et al., *Review of Particle Physics (RPP)*, Phys.Rev. **D86** (2012), 010001.
- [60] G. Isidori, V. S. Rychkov, A. Strumia, and N. Tetradis, *Gravitational corrections to standard model vacuum decay*, Phys.Rev. **D77** (2008), 025034, 0712.0242.
- [61] G. Isidori, G. Ridolfi, and A. Strumia, *On the metastability of the standard model vacuum*, Nucl.Phys. **B609** (2001), 387–409, hep-ph/0104016.
- [62] V. Branchina and E. Messina, *Stability, Higgs Boson Mass and New Physics*, (2013), 1307.5193.
- [63] EPIC Collaboration, J. Bock et al., *Study of the Experimental Probe of Inflationary Cosmology (EPIC)-Intermediate Mission for NASA’s Einstein Inflation Probe*, (2009), 0906.1188.
- [64] COre Collaboration, F. Bouchet et al., *COre (Cosmic Origins Explorer) A White Paper*, (2011), 1102.2181.

- [65] V. Silveira and A. Zee, *SCALAR PHANTOMS*, Phys.Lett. **B161** (1985), 136.
- [66] J. McDonald, *Gauge singlet scalars as cold dark matter*, Phys.Rev. **D50** (1994), 3637–3649, hep-ph/0702143.
- [67] C. Burgess, M. Pospelov, and T. ter Veldhuis, *The Minimal model of non-baryonic dark matter: A Singlet scalar*, Nucl.Phys. **B619** (2001), 709–728, hep-ph/0011335.
- [68] H. Davoudiasl, R. Kitano, T. Li, and H. Murayama, *The New minimal standard model*, Phys.Lett. **B609** (2005), 117–123, hep-ph/0405097.
- [69] B. Patt and F. Wilczek, *Higgs-field portal into hidden sectors*, (2006), hep-ph/0605188.
- [70] D. H. Lyth and E. D. Stewart, *Thermal inflation and the moduli problem*, Phys.Rev. **D53** (1996), 1784–1798, hep-ph/9510204.
- [71] A. R. Liddle and S. M. Leach, *How long before the end of inflation were observable perturbations produced?*, Phys.Rev. **D68** (2003), 103503, astro-ph/0305263.
- [72] A. Hebecker, S. C. Kraus, D. Lust, S. Steinfurt, and T. Weigand, *Fluxbrane Inflation*, Nucl.Phys. **B854** (2012), 509–551, 1104.5016.
- [73] A. Hebecker, S. C. Kraus, M. Kuntzler, D. Lust, and T. Weigand, *Fluxbranes: Moduli Stabilisation and Inflation*, JHEP **1301** (2013), 095, 1207.2766.
- [74] H. Kawai, D. Lewellen, and S. Tye, *A Relation Between Tree Amplitudes of Closed and Open Strings*, Nucl.Phys. **B269** (1986), 1.
- [75] W. Lerche, D. Lust, and A. Schellekens, *Chiral Four-Dimensional Heterotic Strings from Selfdual Lattices*, Nucl.Phys. **B287** (1987), 477.
- [76] I. Antoniadis, C. Bachas, and C. Kounnas, *Four-Dimensional Superstrings*, Nucl.Phys. **B289** (1987), 87.
- [77] K. A. Meissner and H. Nicolai, *Conformal Symmetry and the Standard Model*, Phys.Lett. **B648** (2007), 312–317, hep-th/0612165.
- [78] H. Kawai and T. Okada, *Solving the Naturalness Problem by Baby Universes in the Lorentzian Multiverse*, Prog.Theor.Phys. **127** (2012), 689–721, 1110.2303.
- [79] L. J. Hall and Y. Nomura, *A Finely-Predicted Higgs Boson Mass from A Finely-Tuned Weak Scale*, JHEP **1003** (2010), 076, 0910.2235.
- [80] N. Itzhaki and E. D. Kovetz, *Inflection Point Inflation and Time Dependent Potentials in String Theory*, JHEP **0710** (2007), 054, 0708.2798.
- [81] R. Allahverdi, B. Dutta, and A. Mazumdar, *Attraction towards an inflection point inflation*, Phys.Rev. **D78** (2008), 063507, 0806.4557.
- [82] M. Badziak and M. Olechowski, *Volume modulus inflection point inflation and the gravitino mass problem*, JCAP **0902** (2009), 010, 0810.4251.
- [83] K. Enqvist, A. Mazumdar, and P. Stephens, *Inflection point inflation within supersymmetry*, JCAP **1006** (2010), 020, 1004.3724.
- [84] S. Hotchkiss, A. Mazumdar, and S. Nadathur, *Inflection point inflation: WMAP constraints and a solution to the fine-tuning problem*, JCAP **1106** (2011), 002, 1101.6046.

- [85] S. Hotchkiss, A. Mazumdar, and S. Nadathur, *Observable gravitational waves from inflation with small field excursions*, JCAP **1202** (2012), 008, 1110.5389.
- [86] A. Chatterjee and A. Mazumdar, *Tuned MSSM Higgses as an inflaton*, JCAP **1109** (2011), 009, 1103.5758.
- [87] S. Choudhury and A. Mazumdar, *An accurate bound on tensor-to-scalar ratio and the scale of inflation*, (2013), 1306.4496.
- [88] L. Wang, E. Pukartas, and A. Mazumdar, *Visible sector inflation and the right thermal history in light of Planck data*, JCAP **1307** (2013), 019, 1303.5351.
- [89] S. Choudhury, A. Mazumdar, and S. Pal, *Low & High scale MSSM inflation, gravitational waves and constraints from Planck*, JCAP **07** (2013), 041, 1305.6398.
- [90] M. Veltman, *The Infrared - Ultraviolet Connection*, Acta Phys.Polon. **B12** (1981), 437.
- [91] J. J. Atick and E. Witten, *The Hagedorn Transition and the Number of Degrees of Freedom of String Theory*, Nucl.Phys. **B310** (1988), 291–334.